Japanese Journal of Applied Physics
Vol. 45, No. 46, 2006, pp. L1226–L1229



# Simultaneous Determination of Carrier Concentration, Mobility, and Thickness of SiC Homoepilayers by Infrared Reflectance Spectroscopy

Shingo OISHI[1*], Yasuto HIJIKATA[1], Hiroyuki YAGUCHI[1] and Sadafumi YOSHIDA[1,2†]

[1]*Division of Mathematics, Electronics and Information, Saitama University, 255 Shimo-Okubo, Sakura-ku, Saitama 338-8570, Japan*
[2]*Power Electronics Research Center, National Institute of Advanced Industrial Science and Technology (AIST), Tsukuba Central 2, 1-1-1 Umezono, Tsukuba, Ibaraki 305-8568, Japan*

(Received July 21, 2006; accepted October 10, 2006; published online November 17, 2006)

We have simultaneously determined the carrier concentration, mobility, and thickness of 4H–SiC homoepilayers with carrier concentrations of $10^{17}$–$10^{18}\,cm^{-3}$ from infrared reflectance measurements with the wave number range of $80-2000\,cm^{-1}$. A modified classical dielectric function model was employed for the fitting analyses. We have prepared *n*-type epilayers on *p*-type and *n*-type substrates for comparison with the values of the carrier concentration and mobility estimated from infrared reflectance measurements with those obtained from Hall-effect measurements and *C*–*V* measurements. Through these comparisons, we have confirmed the validity of the values estimated from infrared reflectance measurements.
[DOI: 10.1143/JJAP.45.L1226]

KEYWORDS: SiC, homoepilayer, infrared reflectance, nondestructive and contactless measurement, carrier concentration, mobility, Hall-effect measurement, capacitance–voltage measurement

Silicon carbide (SiC) is an attractive semiconductor for high-temperature, high-power, and high-frequency electronic devices because of its physical properties such as wide band gap, high saturated-electron drift velocity, and high-breakdown electric field. To characterize the electrical properties of semiconductors, electrical measurement techniques such as Hall-effect measurements, and capacitance–voltage (*C*–*V*) measurements have been widely used. For device process monitoring, however, Hall-effect measurements cannot be used because they require the formation of electrodes on samples. *C*–*V* measurements can avoid the formation of electrodes by using a mercury probe as the Schottky contact, but this determines only the net doping concentration, not the carrier concentration. In addition, the use of a mercury probe has the problem of contamination of the sample surface.

In contrast, optical measurement techniques such as Raman scattering spectroscopy,[1–4] infrared spectroscopic ellipsometry,[5] optical absorption measurements,[6] and infrared reflectance measurements[7] have been used as nondestructive and contactless methods to characterize the carrier concentrations of SiC wafers.

Infrared reflectance spectroscopy has also been reported to be able to derive the effective mass of SiC[8,9] and the thickness of homoepitaxially grown SiC layers.[10–12] We have used infrared reflectance spectroscopy to measure the mapping of the carrier concentration and mobility over 2 inch 6H–SiC wafers.[13] By comparison with the results from Hall-effect measurements, we have confirmed the validity of the derivation of the carrier concentration and mobility of SiC wafers from infrared reflectance measurements. Then, we characterized the electrical activation of doped impurities and residual damage in ion-implanted and postannealed 4H–SiC epitaxial layers.[14]

Since homoepilayers are used for the fabrication of SiC electronic devices in general, it is necessary to monitor the carrier concentration and mobility of the homoepilayers, as well as the thickness, in device fabrication processes. It has been recently reported that the electrical properties of epilayers can be estimated by Raman scattering spectroscopy using a deep ultraviolet light source whose penetration depth is extremely small.[15] However, Raman scattering measurements cannot give information on the thickness of epilayers.

In this report, we propose a method for the simultaneous determination of the electrical properties, i.e., the free-carrier concentration, mobility, and thickness of SiC epilayers grown on SiC substrates by infrared reflectance measurements. First, we compare the electrical properties derived from infrared reflectance analyses with those of Hall-effect measurements for *n*-type epilayers grown on *p*-type substrates, and then with those of *C*–*V* measurements in the case of *n*-type epilayers on *n*-type substrates, in order to check the validity of the proposed method.

Samples used in this study were nitrogen-doped *n*-type 4H–SiC epilayers grown on *n*- and *p*-type 4H–SiC substrates supplied from the National Institute of Advanced Industrial Science and Technology. The epilayers were grown on the 4H–SiC(0001) Si face 8° off the substrates by chemical vapor deposition (CVD). The details of the epilayer growth have been described elsewhere.[16] In the case of *n*-type epilayers on *p*-type substrates, the carrier concentration of the epilayers was in the range between $3 \times 10^{17}$ and $2 \times 10^{18}\,cm^{-3}$, and that of the substrates was typically $4 \times 10^{16}\,cm^{-3}$. On the other hand, in the case of *n*-type epilayers on *n*-type substrates, the net doping concentration ($N_D - N_A$) of the epilayers was in the range between $1 \times 10^{17}$ and $8 \times 10^{17}\,cm^{-3}$, and that of the substrates was typically $5 \times 10^{18}\,cm^{-3}$. The thicknesses of the epilayers were 6–7 μm, measured by scanning electron microscopy (SEM) observation of a cleaved facet of the samples.

The infrared reflectance spectra were measured at room temperature (RT) using two Fourier-transform infrared (FTIR) spectrometers, JASCO FT/IR-VM7 for the far-infrared spectral region ($80-650\,cm^{-1}$) and JASCO Irtron IRT-30 infrared microscope for the mid-infrared spectral region ($540-2000\,cm^{-1}$). In the far-infrared region, two light sources (a mercury arc lamp and a nichrome light source), two beam splitters (4- and 12-μm-thick Mylar films) and a pyroelectric deuterated triglycine sulfate (p-DTGS)

*E-mail address: oishi@opt.ees.saitama-u.ac.jp
†E-mail address: yoshida@opt.ees.saitama-u.ac.jp

detector were used. In the mid-infrared region, a high-intensity ceramic light source, a KBr beam splitter, and a mercury cadmium telluride (MCT) detector were used. The diameter of the incident beam used and the wave number resolution for the far-infrared measurements and mid-infrared measurements were 5 mm and 1 $cm^{-1}$, and 0.1 mm and 2 $cm^{-1}$, respectively. In the reflectance measurements, an aluminum mirror was used as a reference.

Hall-effect measurements were performed at RT using the van der Pauw method for *n*-type epilayers on *p*-type substrates. Ohmic contacts were fabricated on the epilayer surfaces by the electron-beam evaporation of Ni and subsequent annealing at 900 °C for 30 min in $N_2$ atmosphere. *C–V* measurements were performed at RT using gold electrodes evaporated on the sample surface as Schottky contacts.

The carrier concentration and mobility of epilayers and substrates, as well as the thickness of the epilayers can be determined simultaneously by fitting the calculated reflectance spectrum to the measured spectrum. The reflectance $R$ of an epilayer on a substrate at normal incidence is given by

$$R = \left| \frac{r_1 + r_2 e^{-2i\delta}}{1 + r_1 r_2 e^{-2i\delta}} \right|^2, \tag{1}$$

where $r_1$ and $r_2$ are the Fresnel reflection coefficients at the air/epilayer and the epilayer/substrate interface, respectively, given by the function of the optical constants of the epilayer and the substrate, and the thickness. The optical constants of SiC in the infrared region are derived from the dielectric constants as a function of the wave number of the incident light as

$$\epsilon(\omega) = \epsilon_\infty \left( \frac{\omega_L^2 - \omega^2 - i\Gamma_L\omega}{\omega_T^2 - \omega^2 - i\Gamma_T\omega} - \frac{\omega_p^2}{\omega^2 + i\gamma_p\omega} \right), \tag{2}$$

where $\epsilon_\infty$ is the high-frequency dielectric constant, $\omega_T$ and $\omega_L$ are transverse optical (TO) and longitudinal optical (LO) phonon frequencies and $\Gamma_T$ and $\Gamma_L$ are the TO and LO phonon damping constants, respectively. The first term in eq. (2) is the contribution from the lattice vibration, where the contributions from the TO phonon damping constant and the LO phonon damping constant are independent of each other.[17] This dielectric function model is called as a modified classical dielectric function (MDF) model. The second term in the equation is related to the plasma oscillation of free carriers, where the plasma frequency $\omega_p$ is given as

$$\omega_p = \sqrt{\frac{Ne^2}{m^*\epsilon_\infty}}, \tag{3}$$

where $N$, $m^*$, and $e$ are the free-carrier concentration, effective mass, and electron charge, respectively. Since the free-carrier damping constant $\gamma_p$ is given by the inverse of the scattering time $\tau$, the free-carrier mobility is derived using

$$\mu = \frac{e}{m^*\gamma_p}. \tag{4}$$

We calculated the infrared reflectance as a function of the wave number using eq. (1). We fitted the calculated spectrum to the measured one by adjusting the values of $\omega_p$, $\gamma_p$, $\Gamma_T$, and $\Gamma_L$ of the epilayer and the substrate, and the epilayer thickness $d$. From these values, we obtained the carrier concentration $N$ and mobility $\mu$ of the epilayer and substrate using eqs. (3) and (4). We adopted the values $\epsilon_\infty = 6.56$, $\omega_T = 798\,cm^{-1}$, $\omega_L = 970\,cm^{-1}$, $m^*_{M\Gamma} = 0.58m_0$, and $m^*_{MK} = 0.31m_0$, obtained from Raman scattering measurements of 4H–SiC[1] and optical detection of cyclotron resonance (ODCR).[18] Considering that the free carriers distribute themselves in proportion to the square root of each effective mass, the averaged effective masses, $m^* = (m^*_{MK} \cdot m^*_{M\Gamma})^{1/2}$ and $m^* = [1/(m^*_{MK})^{1/2} + 1/(m^*_{M\Gamma})^{1/2}]/[1/(m^*_{MK})^{3/2} + 1/(m^*_{M\Gamma})^{3/2}]$, were used for the calculation of the carrier concentration and mobility, respectively.

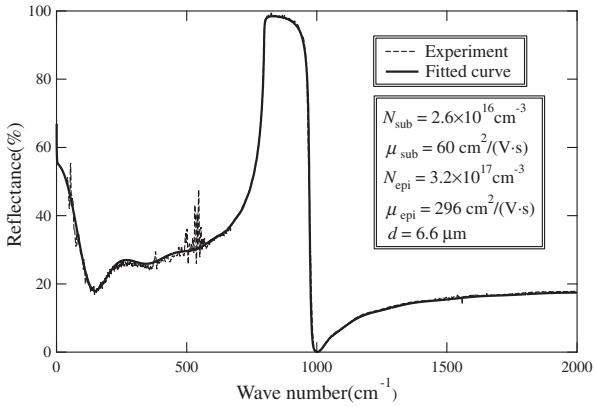


Fig. 1. Infrared reflectance spectrum of an *n*-type epilayer on a *p*-type substrate at room temperature denoted by dashed line. The solid line shows the fitted curve calculated using the MDF model. The values estimated from this fitting analysis are listed in the figure.

First, we estimated the carrier concentration and mobility of *n*-type epilayers on *p*-type substrates from reflectance measurements, and compared them with the values obtained from Hall-effect measurements. Figure 1 shows a typical infrared reflectance spectrum measured for an *n*-type epilayer on a *p*-type substrate. The solid line denotes the calculated values fitted to the experimental values shown as the dashed line. The calculated spectrum was fitted to the observed one by eye. The values $N_{epi} = 3.2 \times 10^{17}\,cm^{-3}$, $\mu_{epi} = 296\,cm^2/(V\cdot s)$, and $d = 6.60\,\mu m$ were obtained by curve-fitting analysis. These values are listed in the figure. In the case of a *p*-type substrate whose carrier concentration is low in general, the reflectance spectrum is almost independent of the electrical properties of the substrate, thus, it is difficult to estimate the carrier concentration and mobility of the substrate. Thus, we have used values for the *p*-type substrate without the epilayer obtained from Hall-effect measurements. The thicknesses of the epilayer obtained from infrared reflectance measurements and those measured from SEM observation coincide with each other within ±1%.

The carrier concentrations and mobilities obtained from infrared reflectance measurements are plotted with respect to those obtained from Hall-effect measurements in Figs. 2(a) and 2(b), respectively. Since the Hall scattering factor $r_H$ is reported to be approximately unity at RT for 4H–SiC,[19,20] we directly compared the drift mobilities estimated from infrared reflectance measurements and the Hall mobilities obtained from Hall-effect measurements. The error bars shown in the figures represent the accuracy of the fitting

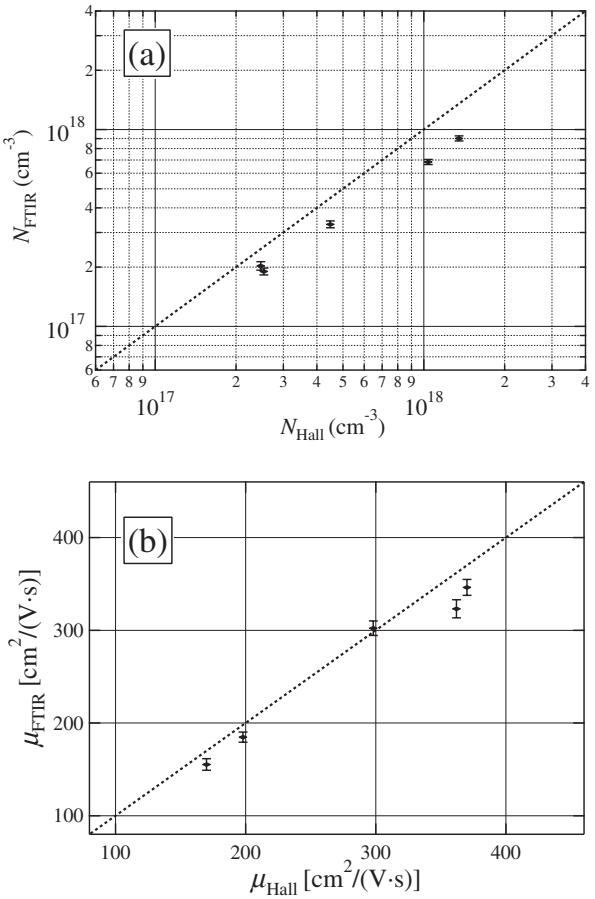


Fig. 2. Values of (a) carrier concentration and (b) mobility estimated from infrared reflectance measurements and Hall-effect measurements. The dotted line in the figures corresponds to $N_{Hall} = N_{FTIR}$ and $\mu_{Hall} = \mu_{FTIR}$ for (a) and (b), respectively, as guides to the eye.

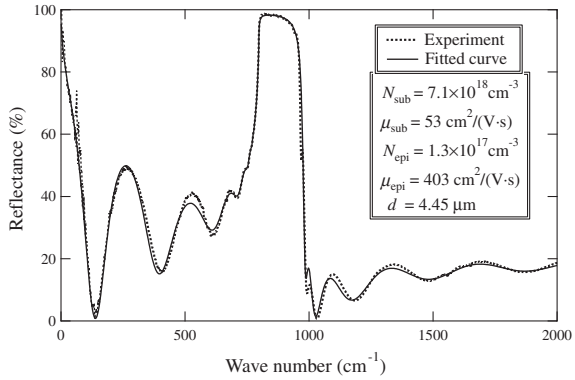


Fig. 3. Infrared reflectance spectrum of an *n*-type epilayer on an *n*-type substrate at room temperature denoted by dashed line. The solid line shows the fitted curve calculated using the MDF model. The values estimated from this fitting analysis are listed in the figure.

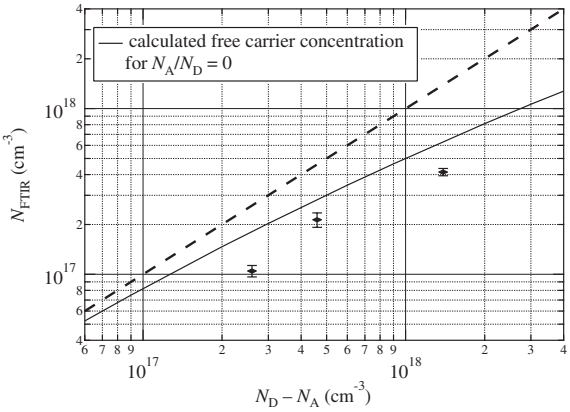


Fig. 4. Values of the carrier concentration estimated from the infrared reflectance for *n*-type epilayers on *n*-type substrates as a function of dopant concentration obtained from *C–V* measurements for each sample. The solid line represents the theoretical carrier concentration for $T = 300$ K assuming zero doping concentration ($N_A = 0$) using eq. (5a). The dotted line represents $N_{FTIR} = N_D - N_A$ as a guide to the eye.

analysis, and the accuracy is about ±4% for both the carrier concentration and the mobility, whereas the accuracy of the values derived from Hall-effect measurements is about ±10%. As can be seen from these figures, the electrical properties obtained from the reflectance spectra are in good agreement with those obtained from Hall-effect measurements. These results suggest that the proposed method is valid for obtaining the values of carrier concentration and mobility of the epilayers. However, careful observation confirms that the values of carrier concentration and mobility derived from infrared reflectance measurements are slightly lower than those obtained from Hall-effect measurements. The difference can be explained by the consideration that the part of the free carriers trapped in defects or bounded by dopants cannot follow in the THz frequency range used for reflectance measurements, unlike in Hall-effect measurements, where a direct current is supplied.

Next, we estimated the values of carrier concentration and mobility for *n*-type epilayers on *n*-type substrates from the infrared reflectance spectra measured. Figure 3 shows a typical infrared reflectance spectrum observed and its fitted curve. The values $N_{epi} = 1.3 \times 10^{17}\,\mathrm{cm}^{-3}$, $\mu_{epi} = 403\,\mathrm{cm}^2/(\mathrm{V{\cdot}s})$, and $d = 4.45\,\mu\mathrm{m}$; and $N_{sub} = 7.1 \times 10^{18}\,\mathrm{cm}^{-3}$, and $\mu_{sub} = 53\,\mathrm{cm}^2/(\mathrm{V{\cdot}s})$ were obtained by curve-fitting analysis as the parameters of the epilayer and substrate, respectively. The accuracy of the carrier concentration and mobility of epilayers derived from the fitting of the reflectance spectrum is about ±10%. In Fig. 4, the free-carrier concentration estimated from the infrared reflectance spectrum is plotted with respect to the net doping concentration $N_D - N_A$ derived from *C–V* measurements. We calculated the free-carrier concentration $n$ from the net doping concentration using

$$n(T) + N_A = \frac{N(h)}{1 + \{gn(T)/N_C\}\exp[\Delta E(h)/k_B T]} + \frac{N(k)}{1 + \{gn(T)/N_C\}\exp[\Delta E(k)/k_B T]}, \quad (5a)$$

$$N_C = 2M_C\left(\frac{m^*_{d.s.} k_B T}{2\pi\hbar^2}\right)^{3/2}, \quad (5b)$$

where $k_B$ is the Boltzmann constant, $T$ is the temperature, $N_A$ is the concentration of acceptors, and $N(h)$ and $N(k)$ are the concentrations of the nitrogens occupied at hexagonal and cubic lattice sites, respectively. Since the number of hexagonal sites is equal to the number of cubic sites for 4H–SiC, the donor concentration $N_D$ is given by $N(h) + N(k)$. The values of $\Delta E(h)$ and $\Delta E(k)$ are the ionization energies of the nitrogen donor at hexagonal and cubic lattice sites,

respectively, and $g = 2$ is the spin degeneracy factor. Equation (5b) gives the effective density of states, where $M_C = 3$ is the number of equivalent conduction band minima and $m^*_{d.s.}$ is the density-of-states effective mass. The values of $\Delta E(h)$ and $\Delta E(k)$ were set as 50 and 100 meV, respectively, referring to reported experimental data.[21,22] The values of $m^*_{M\Gamma} = 0.58m_0$, $m^*_{MK} = 0.31m_0$, and $m^*_{ML} = 0.33m_0$ derived from ODCR measurements[18] were adopted. The solid line in Fig. 4 shows the free-carrier concentration calculated as a function of the net doping concentration in the case of $N_A/N_D = 0$ or $N_D/(N_A + N_D) = 1$, because the epilayers we measured are hardly carrier compensated.[23] The values obtained from the infrared reflectance spectra were slightly lower than the calculated values, as in the case for the samples of *n*-type epilayers on *p*-type substrates. The value of drift mobility calculated in consideration of five carrier-scattering mechanisms[24] was 430 $cm^2/(V \cdot s)$, in the case of $N_A/N_D = 0$ and $N_D - N_A = 2.7 \times 10^{17}\,cm^{-3}$, which is almost the same as the value obtained from the infrared reflectance spectrum, i.e., 403 $cm^2/(V \cdot s)$. This result also indicates that the compensation of the sample is low.

We have performed infrared reflectance measurements in the range between 80–2000 $cm^{-1}$ for epilayers with a carrier concentration in the range of $10^{17}$–$10^{18}\,cm^{-3}$, and have shown that the values of carrier concentration, mobility, and epilayer thickness can be estimated with high accuracy. It is difficult to apply this method to epilayers having carrier concentrations less than $10^{17}\,cm^{-3}$ due to the restriction of the spectral region for the FTIR spectrometer (80 $cm^{-1}$) that we used, and because of the restriction in the carrier concentration range, our method can be applied to only certain epilayers in some SiC devices such as channel layers of MESFETs and electrode contact layers. In order to expand the applicable SiC device area, particularly for devices with a high breakdown voltage, it is necessary to extend to the range of carrier concentrations to less than $10^{17}\,cm^{-3}$. To overcome this problem, an extension of the spectral range of the reflectance measurements to the THz region may be required. In the case of carrier concentrations higher than $10^{19}\,cm^{-3}$, it is also difficult to estimate the electrical properties from the reflectance spectra with high accuracy, as mentioned in our previous paper.[13] It is necessary to derive a novel dielectric function model that takes into account the LO phonon–plasmon coupling.

We have proposed a method for the simultaneous determination of the carrier concentration, mobility, and thickness of SiC homoepilayers using infrared reflectance spectroscopy. Infrared reflectance spectra with a wave number range between 80–2000 $cm^{-1}$ were measured for *n*-type 4H–SiC epilayers on *p*-type and *n*-type 4H–SiC substrates with different carrier concentrations at RT. We estimated the carrier concentration and mobility by curve-fitting using the MDF model. These values of electrical properties for *n*-type epilayers on *p*-type substrates were compared with the values of Hall-effect measurements, and those for *n*-type epilayers on *n*-type substrates were compared with the values of *C*–*V* measurements. Through these comparisons, we have shown that the characterization method using infrared reflectance measurements can determine the electrical properties and the thickness of SiC homoepilayers accurately.

## Acknowledgments

We would like to acknowledge Dr. K. Kojima of the National Institute of Advanced Industrial Science and Technology (AIST) for supplying the SiC epilayer samples and also for valuable comments. We also thank Dr. Y. Ishida and Mr. S. Kuroda of AIST for their valuable discussions and cooperation throughout this study. We thank Professor S. Onari and Associate Professor K. Matsuishi of the University of Tsukuba for providing the Fourier-transform infrared spectrometer. This work is partly supported by an Industrial Technology Research Grant Program for 2004–2006 from the New Energy and Industrial Technology Development Organization (NEDO) of Japan and the Ministry of Education, Culture, Sports, Science and Technology (MEXT) of Japan through a Grant-in-Aid for Young Scientist Research (B) (No. 17760247).

1) H. Harima, S. Nakashima and T. Uemura: J. Appl. Phys. **78** (1995) 1996.
2) J. C. Burton, L. Sun, M. Pophristic, S. J. Lukacs, F. H. Long, Z. C. Feng and I. T. Ferguson: J. Appl. Phys. **84** (1998) 6268.
3) M. Chafai, A. Jaouhari, A. Torres, R. Antón, E. Martín, J. Jiméz and W. C. Mitchel: J. Appl. Phys. **90** (2001) 5211.
4) H. Yagami, S. Nakashima, A. Mitsuishi, A. Uemoto, K. Furukawa, A. Suzuki and S. Nakajima: J. Appl. Phys. **61** (1987) 354.
5) T. E. Tiwald, J. A. Woollam, S. Zollner, J. Christiansen, R. B. Gregory, T. Wetteroth, S. R. Wilson and A. R. Powell: Phys. Rev. B **60** (1999) 11464.
6) R. Weingärtner, P. J. Wellmann, M. Bickermann, D. Hofmann, T. L. Straubinger and A. Winnacker: Appl. Phys. Lett. **80** (2002) 70.
7) H. Yaguchi, K. Narita, Y. Hijikata, S. Yoshida, S. Nakashima and N. Oyanagi: Mater. Sci. Forum **389–393** (2002) 621.
8) M. A. Il'in, A. A. Kukharskii, E. P. Rashevskaya and V. K. Subashiev: Sov. Phys. Solid State **13** (1978) 2078.
9) A. V. Mel'nichuk and Yu. A. Pasechnik: Sov. Phys. Solid State **34** (1992) 227.
10) R. T. Holm, P. H. Klein and P. E. R. Nordquist, Jr.: J. Appl. Phys. **60** (1986) 1479.
11) M. F. Macmillan, A. Henry and E. Janzen: J. Electron. Mater. **27** (1998) 300.
12) M. F. Macmillan, P. O. Narfgren, A. Henry and E. Janzen: Mater. Sci. Forum **264–268** (1998) 645.
13) K. Narita, Y. Hijikata, H. Yaguchi, S. Yoshida and S. Nakashima: Jpn. J. Appl. Phys. **43** (2004) 5151.
14) K. Narita, Y. Hijikata, H. Yaguchi, S. Yoshida, J. Senzaki and S. Nakashima: Mater. Sci. Forum **457–460** (2004) 905.
15) S. Nakashima, H. Okumura, T. Yamamoto and R. Shimizu: Appl. Spectrosc. **58** (2004) 224.
16) K. Kojima, T. Suzuki, S. Kuroda, J. Nishio and K. Arai: Jpn. J. Appl. Phys. **42** (2003) L637.
17) S. Nakashima and H. Harima: J. Appl. Phys. **95** (2004) 3541.
18) D. Volm, B. K. Meyer, D. M. Hofmann, W. M. Chen, N. T. Son, C. Persson, U. Lindefelt, O. Kordina, E. Sorman, A. O. Konstantinov, B. Monemar and E. Janzen: Phys. Rev. B **53** (1996) 15409.
19) G. D. Chen, J. Y. Lin and H. X. Jiang: Appl. Phys. Lett. **68** (1996) 1341.
20) G. Rutsch, R. P. Devaty, W. J. Choyke, D. W. Langer and L. B. Rowland: J. Appl. Phys. **84** (1998) 2062.
21) W. Götz, A. Schöner, G. Pensl, W. Suttrop, W. J. Choyke, R. Stein and S. Leibenzeder: J. Appl. Phys. **73** (1993) 3332.
22) M. A. Capano, J. A. Cooper, Jr., M. R. Melloch, A. Saxler and W. C. Mitchel: J. Appl. Phys. **87** (2000) 8773.
23) J. Nishio, M. Kushibe, K. Masahara, K. Kojima, T. Oono, Y. Ishida, T. Takahashi, T. Suzuki, T. Tanaka, S. Yoshida and K. Arai: Mater. Sci. Forum **389–393** (2002) 215.
24) H. Iwata and K. M. Itoh: J. Appl. Phys. **89** (2001) 6228.